



# Reliability analysis of tunnel lining considering soil spatial variability

Xiangfeng Guo, Dianchun Du, Daniel Dias

## ► To cite this version:

Xiangfeng Guo, Dianchun Du, Daniel Dias. Reliability analysis of tunnel lining considering soil spatial variability. Engineering Structures, 2019, 196, pp.109332 -. <10.1016/j.engstruct.2019.109332>. <hal-03484520>

**HAL Id: hal-03484520**

**<https://hal.science/hal-03484520v1>**

Submitted on 20 Dec 2021

**HAL** is a multi-disciplinary open access archive for the deposit and dissemination of scientific research documents, whether they are published or not. The documents may come from teaching and research institutions in France or abroad, or from public or private research centers.

L'archive ouverte pluridisciplinaire **HAL**, est destinée au dépôt et à la diffusion de documents scientifiques de niveau recherche, publiés ou non, émanant des établissements d'enseignement et de recherche français ou étrangers, des laboratoires publics ou privés.



Distributed under a Creative Commons CC BY-NC 4.0 - Attribution - Non-commercial use - International License

# Reliability analysis of tunnel lining considering soil spatial variability

Xiangfeng GUO<sup>1</sup>, Dianchun DU<sup>1\*</sup>, Daniel DIAS<sup>2,3</sup>

<sup>1</sup> Univ. Grenoble Alpes, CNRS, Grenoble INP\*\*, 3SR, F-38000 Grenoble, France

<sup>2</sup> School of Automotive and Transportation Engineering, Hefei University of Technology, Hefei, China

<sup>3</sup> Antea Group, 92160 Antony, France

\*Corresponding author: [dianchun.du@3sr-grenoble.fr](mailto:dianchun.du@3sr-grenoble.fr)

\*\*Institute of Engineering Univ. Grenoble Alpes

## Abstract

Reliability analysis of the support lining of a shallow circular tunnel excavated in spatially varying soils is presented in the paper. The soil-structure interaction is considered by using a numerical model named the hyperstatic reaction method (HRM). It can provide the internal forces of the tunnel lining in terms of bending moments ( $M$ ), axial ( $N$ ) and shear forces ( $V$ ). The sparse polynomial chaos expansion (SPCE) in combination with the global sensitivity analysis (GSA) is employed to perform the reliability analysis. This method allows reducing the number of the involved input variables according to their sensitivity indices obtained by GSA, and constructing a rational meta-model with limited calls to the mechanical model. Multiple failure modes in the ultimate limit state (ULS) analysis are considered in this study. The individual and system failure probabilities are all provided. The obtained results show that the exceedance of the bending moment resistance is the most probable failure mode, and that the soil spatial variability has a significant influence on the tunnel lining reliability. In addition, the contribution of different soil properties to the variance of the lining forces and the influence of the autocorrelation length on the lining reliability are discussed.

**Keywords:** reliability analysis; tunnel lining; hyperstatic reaction method; sparse polynomial chaos expansion; global sensitivity analysis; soil spatial variability

## 1 Introduction

It has been well recognized that considerable uncertainties in soil properties such as inherent spatial variability exist in the design or safety assessment of the tunnels excavated in soils. In light of this, various reliability-based analyses of tunnels were performed in recent years [1], [2], [11]–[14], [3]–[10]. Compared to the conventional deterministic methods, these analyses can provide more rational results in terms of the mean and variance of the system response or the failure probability, in which uncertainties are taken into account.

The reliability analysis of tunnels mainly focuses on the excavation-induced instability of the advancing face, the ground movement, the wall convergence and the support structure collapse [8]. In the past decades, many researchers have made contributions to the tunnel reliability analysis covering one of the aforementioned problems by using the First-Order-Reliability-Method (FORM) [1]–[4], the metamodeling technique [5]–[7], [9], the importance sampling method [10] or the point estimate method [11]–[13]. However, these analyses did not consider the interaction between the soil and the tunnel lining. As a result, the tunnel lining reliability analysis remains an issue which deserves more attention but is not widely studied. In the literature, several related studies can be found. Lü et al. [14] proposed a reliability-based design optimization method for a rock tunnel support system. The shotcrete thickness and its installation position can be optimized by using this method according to the corresponding reliability index computed from the FORM combined with the response surface methodology (RSM). Hamrouni et al. [8] presented a probabilistic study of a circular tunnel excavated in a soil mass, in which the limit states concerning the surface settlement and the tunnel lining bending moment were considered. The reliability index of the tunnel was computed by the FORM with RSM. Kroetz et al. [15] investigated the tunnel lining reliability by using the HRM. The soil

was assumed to be homogeneous and simulated by means of random variables. Five individual failure modes, associated with the lining forces, were assessed in the reliability analysis by using the FORM, the crude Monte Carlo Simulation (MCS), the Subset Simulation (SS) and the Importance Sampling method (IS). All the previous works provided interesting insights into the tunnel lining reliability, and showed the necessity of probabilistic analysis. However, some limitations can be figured out from these studies. Firstly, the soil spatial variability was ignored in the three studies mentioned above. The authors used random variables (RVs) approach to describe the soil mass variability. However, this is not realistic since the soil properties vary spatially, even within one soil layer, due to the depositional and post-depositional processes [16]. Secondly, some important soil properties were treated as constants in the probabilistic analysis in [8], such as the earth lateral ground pressure coefficient. Consequently, the uncertainties in soil mass were not completely described. Thirdly, only one failure mode of the tunnel lining (bending moment criterion) was considered in [8]; only the system failure of the tunnel lining was investigated in [14]. Therefore, the contribution of each individual failure mode to the system failure remains unknown.

This paper is dedicated to analysing the tunnel lining reliability by taking into account the soil spatial variability. It aims at investigating the influence of this soil inherent characteristic on the tunnel lining reliability in terms of individual and system failure modes. The tunnel lining and the limit state functions proposed in [15] are adopted in this study. The deterministic calculation is performed by using HRM as in [15]. The originality of this work is the fact that HRM is coupled with the random field theory to consider soil spatial variability. The propagation of the uncertainties in the soil properties is quantified by a metamodeling-based MCS. The meta-model used to perform the MCS is constructed by an approach named SPCE/GSA which combines the sparse PCE with a global sensitivity analysis. This technique is more efficient than

a direct MCS on the deterministic model and is able to provide more interesting results than other reliability methods such as the FORM, SS and IS which are targeted particularly to compute the failure probability. The results available in the SPCE/GSA include the failure probability, the distribution and statistical moments of the model response and the sensitivity index of each input random variable [9], [17].

The paper starts with a brief introduction to the mathematical and mechanical tools used for the reliability analyses including the deterministic model (i.e. the HRM), the Karhunen–Loève (K-L) expansions for the random field simulation and the metamodeling technique SPCE/GSA. It is followed by the problem statement in which the studied tunnel lining is described; the limit state functions are defined and the parameters for the soil properties are presented. A procedure of using the HRM, the K-L expansion and the SPCE/GSA for assessing the tunnel lining reliability is provided as well. Thereafter, a parametric study is performed. The aim is to investigate the impact of each soil property on the variation of the lining forces and to reduce eventually the number of the soil properties that will be simulated with random fields in the following analyses. Then, the tunnel lining reliability is studied by following the procedure mentioned before with the soil properties selected in the parametric study. The effects of the autocorrelation length and of the soil spatial variability are investigated. A section of discussions is presented before the conclusions and two issues are discussed: the computational efficiency of the method SPCE/GSA and the comparison with the previous work [15]. The paper ends with some concluding remarks drawn from the present study which may be useful for the tunnel lining design and analysis.

## 2 Deterministic model and reliability analysis tools

This section aims at presenting all the employed methods for the reliability analysis of the tunnel lining. They include the deterministic model HRM, the reliability method

SPCE/GSA and the random field generation method Karhunen–Loève (K-L) expansion.

## 2.1 Presentation of the HRM

The HRM is an efficient numerical method employed to estimate the soil-structure interactions in a deterministic framework. This method was proposed and improved by Duddeck and Erdmann [18], Takano [19], Oreste [20] and Do et al. [21]. The results of the **lining internal forces** can be quickly obtained by the HRM. Its accuracy has been validated by comparing with numerical simulations (e.g. finite difference method) for homogeneous soils with different types of section (e.g. circular [20], [21] and U-shape [22]) and for layered soils with circular sections [23], [24]. It should be noted that as one requirement of the HRM method, the active loads applied directly to the tunnel structures need to be defined. The following gives a brief description of the HRM. For more details about the HRM, readers can refer to [21].

In the HRM, the tunnel lining is divided into a number of one-dimensional beam elements as shown in Figure 1. Those structural elements are connected to the surrounding soils by means of normal and shear springs of the nodes. Therefore, the interaction between soil and tunnel support is considered through the applied loads (Figure 2) and the springs. In fact, the number of elements has no significant effect on the internal forces when it reaches a certain value. For example, when the number of element is equal to 360, the estimated maximum bending moment is 0.1344 **kN.m/m** while it leads to a slightly smaller one of 0.1343 **kN.m/m** if the number of elements is set equal to 3600. The calculation accuracy is improved by 0.074%, but the calculation time increases from 2.5 seconds to over 270 seconds (on an Intel Xeon CPU E5-2609 v4 1.7GHz (2 processors) PC). Therefore, the number of element is adopted as 360 for the present study.

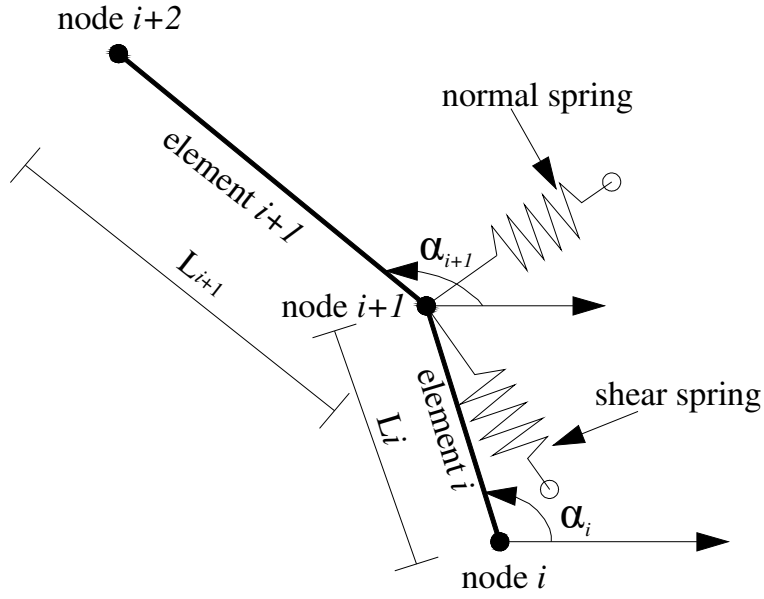


Figure 1. Details of the soil–support interaction through springs connected to the support nodes

According to [20], the focus of the soil–lining interaction problems is to obtain the unknown displacements  $\mathbf{u}_d$  of the discretised structure nodes. The vector of the displacement  $\mathbf{u}_d$  could be evaluated by:

$$\mathbf{K}\mathbf{u}_d = \mathbf{F} \quad (1)$$

where  $\mathbf{K}$  is the global stiffness matrix,  $\mathbf{F}$  is the force vector. The global stiffness matrix  $\mathbf{K}$  could be assembled by the local stiffness matrices of each element on the basis of the criteria described in [25]. The internal forces and displacements of tunnel lining could be calculated once the displacements  $\mathbf{u}_d$  are known.

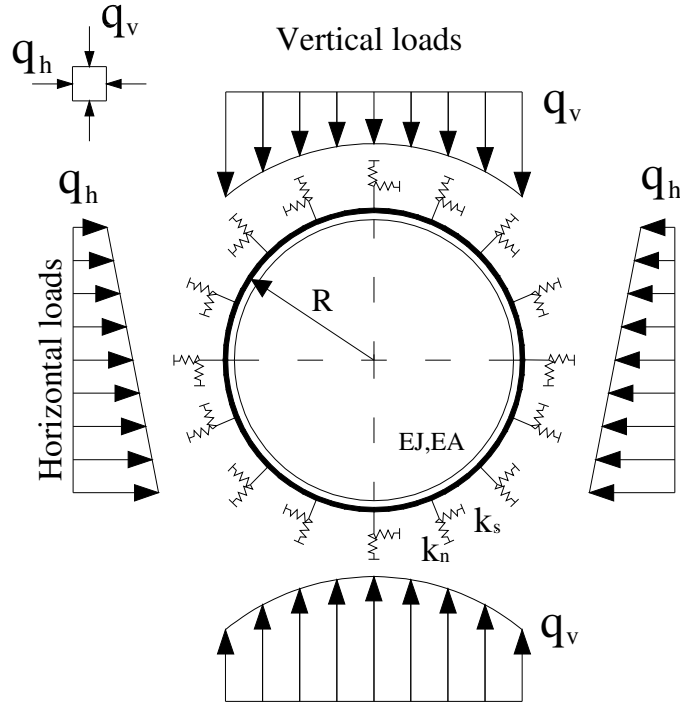


Figure 2. Scheme of tunnel lining, with active vertical and horizontal loads

Notes to Figure 2:  $q_v$ : vertical load;  $q_h$ : horizontal load;  $k_n$ : normal stiffness of the interaction springs;  $k_s$ : tangential stiffness of the interaction springs;  $R$ : tunnel radius;  $EJ$  and  $EA$ : bending and normal stiffness of the lining [21].

### 2.1.1 Soil-structure interaction

As mentioned above, the soil-structure interaction is accomplished through the active loads directly applied on the tunnel structure by the surrounding soil and through the springs connected to the structure nodes. As the active loads are defined, one needs subsequently to determine the stiffness of springs. A non-linear function, which is used to describe the relationship between reaction pressure  $p$  and structure deformation  $\delta$ , was introduced by [20]:

$$p = p_{lim} \left( 1 - \frac{p_{lim}}{p_{lim} + \eta_0 \delta} \right) \quad (2)$$

where  $p_{lim}$  is the maximum reaction pressure offered by the soil, and  $\eta_0$  is the initial stiffness of the soil. The initial normal soil stiffness  $\eta_{n,0}$  depends on the tunnel radius



$R$ , the Poisson's ratio  $\nu_s$  and Young's modulus  $E_s$  of soil. It is estimated by  $\eta_{n,0} = 2 \cdot \frac{E_s}{(1+\nu_s) \cdot R}$  in the analysis. The shear springs of the nodes are considered as well in this study, like the model introduced by [21]. The stiffness of shear spring is approximated to be 1/3 of the normal stiffness [21], as the shear stiffness at the soil-structure interface is difficult to estimate. The values of both the maximum normal reaction pressure  $p_{n,lim}$  and the maximum shear reaction pressure  $p_{s,lim}$  could be estimated by the cohesion  $c$  and the friction angle  $\phi$  of soil. According to [21], they are evaluated by  $p_{n,lim} = \frac{2 \cdot c \cdot \cos\phi}{1 - \sin\phi} + \frac{1 + \sin\phi}{1 - \sin\phi} \cdot \frac{q_v + q_h}{2} \cdot \frac{\nu_s}{1 - \nu_s}$  and  $p_{s,lim} = \frac{q_v + q_h}{2} \cdot \tan\phi$ , respectively.

It is necessary to note that the normal springs would be effective only when the structure moves towards the soil, which means that only the compressive loads are allowed by the normal springs. In contrast, the shear springs could produce both positive and negative stresses along the shear direction.

### 2.1.2 Active loads

The active loads  $q_v$  are estimated by Terzaghi's formula [19] :

$$q_v = \gamma_g h \quad (3)$$

where  $\gamma_g$  represents the soil unit weight and  $h$  is the overburden thickness of the tunnel. If the value of  $h$  is more than two times the external diameter  $D_0$  (Figure 3) of the lining, an effective overburden thickness  $h_0$  ( $h_0 \geq 2D_0$ ) should be used [19]. In addition, the horizontal loads  $q_h$  applied to the tunnel lining in the HRM model are determined by the formula:  $q_h = K_0 \cdot q_v$ , where  $K_0$  is the lateral earth pressure coefficient.

Based on the descriptions above, the HRM performance is considered to be independent to the soil heterogeneity since the divided beam elements (360 beams in this study) and the distributed springs along the lining allow taking into account

different values of a soil property at different locations of the interface. The characteristics of each beam and each spring are determined directly by the contacted soils and may be varied along the lining. This indicates that the soil heterogeneity effect can be well accounted for in the HRM. Therefore, it is effective to couple it with the random field theory which is used to represent the heterogeneity of soils.

## 2.2 Simulation of random fields by the K-L expansion

In this study, the random fields are generated by the K-L expansion method. Consider a stationary Gaussian random field  $H(\mathbf{x}, \boldsymbol{\xi})$  indexed on a bounded domain  $\Omega$ . It can be expressed by the K-L expansion as [26]:

$$H(\mathbf{x}, \boldsymbol{\xi}) = \mu + \sigma \sum_{i=1}^{\infty} \sqrt{\lambda_i} \theta_i(\mathbf{x}) \xi_i \quad (4)$$

where  $\mathbf{x}$  represents the coordinates of an arbitrary point in  $\Omega$ ,  $\mu$  and  $\sigma$  are respectively mean value and standard deviation of the random field,  $\boldsymbol{\xi}$  is a vector of standard uncorrelated random variables which indicates the random nature of the corresponding quantity, and  $\lambda_i$  and  $\theta_i$  are respectively the eigenvalues and eigenfunctions of the autocovariance function of the random field. An autocovariance function is defined as the product of the variance and the autocorrelation function. There are several types of autocorrelation function such as linear, exponential, squared exponential and power autocorrelation functions. An autocorrelation function is able to give the correlation value between two arbitrary points  $(x, y)$  and  $(x', y')$  in  $\Omega$ . In this study, an exponential autocorrelation function is used [27]:

$$\rho(x, y) = \exp\left(-\frac{|x - x'|}{L_x} - \frac{|y - y'|}{L_y}\right) \quad (5)$$

where  $L_x$  and  $L_y$  are respectively the horizontal and vertical autocorrelation length.

In practice, the K-L expansion is truncated to a limited number of series terms. Eq. (4) is then approximated by:

$$H(\mathbf{x}, \boldsymbol{\xi}) = \mu + \sigma \sum_{i=1}^S \sqrt{\lambda_i} \theta_i(\mathbf{x}) \xi_i \quad (6)$$

where  $S$  is the size of the series expansion for the truncated form. The value of  $S$  depends on the desired accuracy, the autocorrelation length ( $L_x, L_y$ ) and dimension of the random field. It can be determined by evaluating the error estimation of the truncated series expansion. The error estimate based on the variance of the truncated error for a K-L expansion with  $S$  terms is given by [28]:

$$\varepsilon = \frac{1}{\Omega} \int_{\Omega} \left[ 1 - \sum_{i=1}^S \lambda_i \theta_i^2(\mathbf{x}) \right] d\Omega \quad (7)$$

In order to obtain a sufficient accuracy in terms of the variance error for random fields, Li and Der Kiureghian [29] recommended that the stochastic grid size of a random field can be set as 0.2 times the autocorrelation length.

In the case of log-normal random fields, the K-L expansion given in Eq. (6) becomes [30]:

$$H(\mathbf{x}, \boldsymbol{\xi}) = \exp \left[ \mu_{ln} + \sigma_{ln} \sum_{i=1}^S \sqrt{\lambda_i} \theta_i(\mathbf{x}) \xi_i \right] \quad (8)$$

where  $\mu_{ln}$  and  $\sigma_{ln}$  are respectively mean value and standard deviation of the log-normal random field.

### 2.3 The reliability method: SPCE/GSA

This subsection describes briefly the reliability method employed in this study. It starts with a presentation of the PCE which is the basis of the SPCE. Then, the SPCE

and the GSA are introduced individually. In the end, the combination of the two methodologies is presented.

### 2.3.1 Polynomial Chaos Expansions (PCE)

The PCE methodology is a powerful tool for metamodeling. It approximates an original model  $\mathbf{D}$  by expanding the model response on a suitable basis which is a series of multivariate polynomials [31]. The PCE can be expressed as follows:

$$Y = \mathbf{D}(\boldsymbol{\zeta}) \cong \sum_{\boldsymbol{\alpha} \in \mathbb{N}^M} k_{\boldsymbol{\alpha}} \Psi_{\boldsymbol{\alpha}}(\boldsymbol{\zeta}) \quad (9)$$

where  $\boldsymbol{\zeta}$  is a vector of independent random variables  $\boldsymbol{\zeta} = \{\zeta_1, \zeta_2, \dots, \zeta_M\}$  with  $M$  representing the number of input variables,  $\Psi_{\boldsymbol{\alpha}}(\boldsymbol{\zeta})$  are multivariate polynomials,  $k_{\boldsymbol{\alpha}}$  are unknown coefficients to be computed and  $\boldsymbol{\alpha} = \{\alpha_1, \dots, \alpha_M\}$  is a multidimensional index. The multivariate polynomial is the tensor product of univariate orthonormal polynomials. In this paper, standard normal random variables in conjunction with the Hermite polynomials are used.

In practice, the representation of the random response in Eq. (9) needs to be truncated to a finite number of terms. In this study, the hyperbolic truncation scheme [32] is adopted to limit the number of involved multivariate polynomials. This truncation scheme defines a so-called q-quasi-norm and requires that the norm is smaller than a given  $p$ . Once the truncated basis is determined, the coefficients  $\{k_{\boldsymbol{\alpha}}\}_{\boldsymbol{\alpha} \in A^{M,p,q}}$  can be computed using the least-square regression method [33]. The accuracy of the PCE can be estimated by the empirical mean-square residual error estimation  $R^2$  and the leave-one-out error estimation  $Q^2$ . Concerning the details of the calculation of these two error estimates, readers are referred to [33].

### 2.3.2 Sparse Polynomial Chaos Expansions (SPCE)

The SPCE was proposed by Blatman and Sudret [32]–[34] in order to limit the number of multivariate polynomials. It is inspired by the fact that the non-zero coefficients in the PCE form a sparse subset of the truncation set [35].

The procedure for building an SPCE is based on an iterative procedure [33]. This procedure is described as follows:

1. Generate randomly an initial experimental design  $\mathcal{X}$  and compute the corresponding model responses  $\hat{\mathbf{Y}}$  by using the deterministic model
2. Determine the user-defined parameters: the target accuracy  $Q_{tg}^2$ , the maximal PCE degree  $P_{max}$  and the cut-off values  $\varepsilon_1, \varepsilon_2$ .
3. For any PCE order  $p \in \{1, \dots, p_{max}\}$ :
  - Forward step: compute the increase in the determination coefficient  $R^2$  by adding each candidate multivariate polynomial from a PCE basis set  $(A^{M,p,q})$ . Retain eventually those candidate terms that lead to a significant increase in  $R^2$ , i.e. greater than  $\varepsilon_1$ . Let  $A^{p,+}$  be the final truncation set at this stage.
  - Backward step: compute the decrease in  $R^2$  by removing each candidate term in  $A^{p,+}$  of then degree not greater than  $p$ . Discard eventually from  $A^{p,+}$  those terms that lead to an insignificant decrease in  $R^2$ , i.e. less than  $\varepsilon_2$ . Let  $A^p$  be the final truncation set.
  - If  $Q_{A^p}^2 \geq Q_{tg}^2$ , stop

In this paper, the following values are selected for the user-defined parameters in the SPCE according to the works in [9], [17]:  $Q_{tg}^2 = 0.99$ ,  $P_{max} = 5$ ,  $\varepsilon_1 = \varepsilon_2 = 5 \times 10^{-5}$  and the q-quasi-norm  $q = 0.7$ .

Using the sparse PCE can improve the efficiency and performance of the PCE since the number of terms (multivariate polynomials) can be significantly reduced in a rational way. It was shown that the sparse PCE can reduce the number of terms from 2024 to 138 for the studied frame structure in [33]. The SPCE has been successfully applied for reliability analysis of benchmark academic examples [33] and various geotechnical engineering problems such as tunnel face stability [36], foundation bearing capacity [31] and earth dam stability [17].

### 2.3.3 Global Sensitivity Analysis (GSA)

The Global sensitivity analysis (GSA) allows quantifying the contribution of each input variable to the variance of the model response [37]. Sudret [37] introduced an analytical way for computing the Sobol index (a type of sensitivity index [38]) as a post-processing of the PCE coefficients. The first order Sobol index can be calculated as follows:

$$S(\zeta_i) = \frac{\sum_{\alpha \in A_{\zeta_i}} (k_j)^2 E[(\Psi_\alpha)^2]}{\sum_{\alpha \in A} (k_j)^2 E[(\Psi_\alpha)^2]} \quad (10)$$

where  $k_j$  are the PCE coefficients,  $A$  is the truncation set ( $A^{M,p,q}$ ),  $A_{\zeta_i}$  is a subset of  $A$  in which the multivariate polynomials  $\Psi_\alpha$  are only functions of the random variable  $\zeta_i$  (i.e., they only contain the variable  $\zeta_i$ ) and  $E[(\Psi_\alpha)^2]$  is the expectation of  $(\Psi_\alpha)^2$ .

### 2.3.4 The combination of the SPCE and GSA

Using SPCE, the computational time was found still important when dealing with problems concerning spatially varying soils, in which 50 ~ 500 random variables from random field discretisation should be considered. In order to address the problem, the SPCE/GSA procedure was proposed in [31], [37]. The main idea is to firstly select the significant input variables by using GSA based on a small order SPCE and then to approximate the system response using a higher order SPCE that only makes use of the selected variables. The input variables with a great value of Sobol index are regarded as significant variables, which forms an effective variables dimension. This dimension is smaller than the initial dimension where the total number of random variables is considered. It should be noted that the PCE order has almost no influence on the Sobol indices, so a PCE with order 2 can accurately provide the contribution of each input variable to the system response variability [31], [37].

As a conclusion, the SPCE/GSA procedure leads to a reduction in the number of the input variables and consequently a limited number of deterministic model calls. The general description of the SPCE/GSA procedure is given as follows:

1. Select the significant input variables by performing a GSA based on a 2<sup>nd</sup>-order SPCE,
2. Construct a meta-model using a high-order SPCE with the selected variables (effective dimension),
3. Perform a Monte-Carlo simulation using the obtained meta-model to compute PDFs of the system response and failure probabilities.

It should be noted that a threshold of 0.98 is adopted to choose the effective variables when performing a GSA with a 2<sup>nd</sup>-order SPCE in step 1. This means that the sum of the selected variables Sobol indices should be bigger than 0.98. Thus, at least 98% of the total variance of the system response can be covered.

The last step of the SPCE/GSA is to perform an MCS w.r.t. the high-order SPCE meta-model. For an MCS with  $N_{MCS}$  model evaluations, the failure probability  $Pf$  can be expressed as follows:

$$Pf = \frac{1}{N_{MCS}} * \sum_{i=1}^{N_{MCS}} I_{MCS} \quad (11)$$

where  $I_{MCS}$  is a failure indicator;  $I_{MCS}$  is set to 1 if the system fails and  $I_{MCS} = 0$  otherwise. The number of  $N_{MCS}$  should be large enough in order to obtain an accurate estimate. The coefficient of variation of  $Pf$  for an MCS can be calculated by [28]:

$$CoV_{Pf} = \sqrt{(1 - Pf)/(N_{MCS} * Pf)} * 100\% \quad (12)$$

## 2.4 Summary of the employed research methods

The previous sections present all the research methods employed in this paper for the purpose of studying the tunnel lining reliability by considering soil spatial variabilities. A numerical approach named HRM is adopted as the deterministic

model to estimate the response of the tunnel support structure. The soil-lining interaction is simulated by various normal and shear springs in the HRM. The uncertainties of soil properties are represented by random fields generated with the K-L expansions in which an autocorrelation function needs to be defined. Then, the propagation of the uncertainties is quantified by a MCS w.r.t. the SPCE meta-model which is an approximation of the HRM response. The MCS allows estimating the failure probability and providing the distribution of the model response. Particularly, a dimension reduction technique (GSA in this paper) is used prior to the construction of a high order SPCE model since a large number of variables should be considered due to the discretization of random fields. This technique is very useful to improve the efficiency of the SPCE for high dimensional stochastic problems. In addition, the combination of the GSA and SPCE can provide an accurate estimate of the failure probability according to a comparative study [39] conducted on an earth dam problem.

### 3 Problem statement

This section aims at presenting the studied tunnel lining and the uncertainties of the soil parameters considered in this study. The limit state functions and the procedure of using the SPCE/GSA in combination with the K-L expansion and the HRM are provided as well.

#### 3.1 Presentation of the tunnel lining

The tunnel lining studied in this paper was firstly proposed in [15] and is shown in Figure 3. It is a circular tunnel with a diameter  $D_0 = 10m$ , an overburden thickness  $h = 20m$ , and a lining thickness  $d_0$  of 0.4m. Following [40], such lining can withstand bending moments of 0.5 MN.m, axial forces of 8.2 MN and shear stresses of 0.75 MN. These values are adopted in the paper to describe the tunnel lining strength. As the present study focuses on the effect of the soil spatial variability, the



367 tunnel lining is assumed to be deterministic. This is based on the fact that the support  
 368 lining is usually made by precast materials which have a low variability in terms of  
 369 mechanical properties when compared to soils which are natural materials and are  
 370 related to a lot of uncertainties [41], [42].

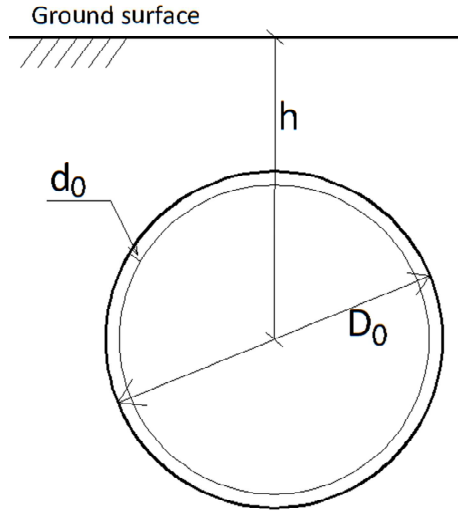


Figure 3. The studied tunnel lining

### 373 3.2 Definition of the limit state functions

374 The strength values mentioned above are used for defining the limit state functions in  
 375 the reliability analyses. In this study, all the possible failure modes of the tunnel lining  
 376 in the ultimate limit state (ULS) are taken into account. With this consideration, five  
 377 limit state functions proposed by [15] are adopted to characterize the tunnel lining  
 378 failure (Eqs.(13) to (17)) , in terms of bending moment ( $M$ ), normal force ( $N$ ) and  
 379 shear force ( $V$ ). The tunnel lining will fail if any of the three internal actions exceeds  
 380 its corresponding capacity (i.e. any limit state function is less than 0).

$$G_1 = 0.5 - \max(\mathbf{M}) \quad (13)$$

$$G_2 = 0.5 + \min(\mathbf{M}) \quad (14)$$

$$G_3 = 8.2 - \max(\mathbf{N}) \quad (15)$$

$$G_4 = 0.75 - \max(\mathbf{V}) \quad (16)$$

$$G_5 = 0.75 + \min(\mathbf{V}) \quad (17)$$

It is noted that the normal force  $N$  is always positive; hence just a single limit state is proposed for  $N$ . Since bending moments  $M$  and shear forces  $V$  can both be either positive or negative, two limit state functions are considered for each internal action.

The effects of the three load types ( $M$ ,  $N$  and  $V$ ) of the tunnel lining response are considered separately with five performance functions. In some cases, their impacts are applied jointly on the support structure. Using individual performance functions may overestimate or underestimate the capacity of the tunnel lining. For example, when considering jointly the  $M$  and  $N$  to determine the tension stress of the lining, the estimated value will be lower than the one obtained with considering only  $M$  since  $N$  always provides compression stresses. In this case, considering individually  $M$  and  $N$  leads to more conservative estimates. In practice, if an interaction equation which jointly accounts for the  $M$ ,  $N$  and  $V$  could be determined, one can then follow the procedure shown in the paper to study the tunnel lining reliability by replacing the five performance functions with only one.

### 3.3 Description of the soil variability

Only the uncertainties of soil properties are accounted for in the proposed reliability analysis. The geometry and resistance of the tunnel lining are considered as deterministic. The most relevant soil properties in tunnel lining design using the HRM are the lateral ground pressure coefficient ( $K_0$ ), the soil cohesion ( $c$ ), the internal friction angle ( $\phi$ ), the Young's modulus ( $E$ ), the Poisson's ratio ( $\nu$ ) and the soil unit weight ( $\gamma_g$ ). The probabilistic statistics and distribution of these soil properties used in [15] are adopted in this study. These values are based on assumptions and published data in the literature [40]–[42]. In addition, the six soil properties are assumed to be uncorrelated as the works in [15]. It is noted that the shape parameters of the Beta distribution for  $\phi$  can be derived from the four parameters given in and below Table 1.

Presenting statistical moments instead of shape parameters for the Beta distribution is more straightforward to have an idea of the value and the variation of  $\phi$ .

In the random field theory, the most important factor is the autocorrelation length. It defines, together with an autocorrelation function, the autocorrelation structure of a random field. According to a literature review given by El-Ramly et al.[43], the autocorrelation length for soils is usually within a range of 10 to 40m in the horizontal direction, while it ranges between 1 and 3m in the vertical direction. In this paper, the autocorrelation is set to 40m and 3m respectively for the horizontal and vertical direction. This choice can lead to a larger failure probability hence a conservative design according to the conclusions in [9], [31], [44]. The influence of using different values of the autocorrelation length on the tunnel lining reliability will be discussed in the section *Numerical simulations and results*.

**Table 1 Probabilistic statistics and distribution of the soil properties**

Variable	Unit	Distribution type	Mean	CoV <sup>(2)</sup> (%)
$K_0$	-	Lognormal	0.9	15
$c$	KPa	Lognormal	4.5	20
$\phi$	Rad	Beta <sup>(1)</sup>	0.35	20
$E$	MPa	Lognormal	60	15
$\nu$	-	Lognormal	0.3	5
$\gamma_g$	MN/m <sup>3</sup>	Lognormal	0.0195	20

Notes: <sup>(1)</sup> the Beta distribution is bounded within a range of [0, 0.78538]; <sup>(2)</sup> CoV: coefficient of variation

### 3.4 Reliability analysis procedure used in the paper

The procedure of the reliability analysis using the SPCE/GSA with the HRM considering the spatial variability of one soil parameter  $T$  necessitates the following steps:

#### A. Generation of random fields

- Prescribe the autocorrelation length and the dimension of the random field.
- Determine the series term  $S$  of the K-L expansion for a desired accuracy by evaluating the error estimate given by Eq. (7).
- Generate  $N_{ED}$  standard normal vectors  $\{\boldsymbol{\zeta}^{(1)}, \boldsymbol{\zeta}^{(2)}, \dots, \boldsymbol{\zeta}^{(N_{ED})}\}$  using the Latin hypercube sampling method. Each vector has a dimension of  $S$ .
- Generate a realisation of random fields for each vector  $\boldsymbol{\zeta}^{(i)}$ . It is obtained, as a consequence,  $N_{ED}$  random fields.

#### B. Evaluation of the internal actions of the tunnel lining

- Determine the value of the soil parameter  $T$  for each beam element in the HRM according to the first random field  $RF_1$  generated previously.
- Perform the HRM to obtain the internal actions of the tunnel lining associated with the  $RF_1$ . The results are written in a vector  $\{\max(\mathbf{M}), \min(\mathbf{M}), \max(\mathbf{N}), \max(\mathbf{V}), \min(\mathbf{V})\}$ .
- Repeat the two previous steps for other generated random fields ( $RF_2$  to  $RF_{N_{ED}}$ ). At the end of this step,  $N_{ED}$  vectors of the results are obtained.
- Reassemble the  $N_{ED}$  vectors of the results to a matrix of  $N_{ED} \times 5$ , donated as  $\mathcal{R}$ .

#### C. Construction of the five meta-models

- Construct a 2<sup>nd</sup>-order SPCE meta-model for the values of  $\max(\mathbf{M})$  following the section 2.3. The  $N_{ED}$  vectors of  $\boldsymbol{\zeta}^{(i)}$  are input random variables and the first column of the matrix  $\mathcal{R}$  is regarded as the model response.
- Compute the Sobol index of each input variable according to the coefficients of the constructed 2<sup>nd</sup>-order SPCE meta-model. Select significant variables based on their Sobol index to form an effective dimension of the input variables.
- Construct a higher-order SPCE meta-model for the values of  $\max(\mathbf{M})$  w.r.t. the selected variables. The dimension of the selected variables is less than the number of initial variables and corresponds to the dimension reduction technique in the SPCE/GSA.
- Repeat the previous three steps to construct other higher-order meta-models respectively for the values of  $\min(\mathbf{M})$ ,  $\max(\mathbf{N})$ ,  $\max(\mathbf{V})$  and  $\min(\mathbf{V})$ .

#### D. Monte Carlo Simulations

- Perform an MCS for each constructed higher-order SPCE meta-model.
- Post-processing on the MCS results to obtain the mean and variance of the five internal actions, individual failure probabilities (Eq. (11)) and the system failure probability.

470

471 If the regression problem cannot be resolved in stage **C** when constructing a meta-  
472 model, a complementary set of input variables ( $\Delta N_{ED}$  vectors of  $\zeta^{(i)}$ ) should be added  
473 to the initial experimental design and then follow the next steps in the procedure. This  
474 work should be repeated until the regression problem is well-posed.

## 475 **4 Parametric analysis**

476 Prior to the reliability analysis of the tunnel lining with random fields, a parametric  
477 analysis is conducted. The objective is to investigate the importance of each soil  
478 property in the reliability analysis. Kroetz et al. [15] has shown that the effects of the  
479 **soil** properties ( $c$ ,  $\phi$ ,  $E$ , and  $\nu$ ) are very limited and can be treated as deterministic  
480 under the assumed probabilistic model (Table 1). However, the work in [15] was  
481 established with means of random variables. When dealing with spatially varying  
482 soils, some parameters along the continuum may impose additional demands to the  
483 lining by itself. The sensitivity indices estimated with the assumption of homogenous  
484 sites for the 6 soil properties may be modified. Therefore, this section aims at  
485 providing insights into the effects of the 6 soil parameters in the framework of random  
486 fields. Firstly, the necessary parameters for the random fields of the 6 soil properties  
487 are determined. Then, a parametric analysis is performed in which the contribution of  
488 each soil property to the variability of the HRM results is presented.

### 489 **4.1 Parameters selection**

490 Figure 4 presents the dimension of the six involved random fields. As presented in  
491 section 2, the interaction between the tunnel lining and the surrounding soil is  
492 simulated by means of normal and shear springs in the HRM. The parameters of the  
493 springs are determined by using only the soil at the soil/lining interface. Therefore, it  
494 is sufficient to use a domain of 10×10m which covers exactly the tunnel to represent  
495 the random fields in HRM calculations. For the  $\gamma_g$ , the random field should be

496 extended to the ground surface in order to take into account the  $\gamma_g$  values at the top of  
 497 the tunnel. The required dimension for  $RF_{\gamma_g}$  is thus 10×20m. Specifically, a  $\Delta d$  of 1m  
 498 is added for each side of the random fields in this paper. Li and Kiureghian [29] has  
 499 shown that the errors of the series expansions methods (e.g. K-L) are large at the  
 500 boundaries of the random fields. Adding a  $\Delta d$  to each side guarantees that the  
 501 simulated values at the soil/lining interface are accurate enough. This technique was  
 502 adopted also in [45] to avoid large errors at the boundaries of the physical random-  
 503 fields domain. In conclusion, the domain of the random field for  $\gamma_g$  is represented by  
 504 the rectangle ABEF (Figure 4) of 12×27m, while the random fields for the other five  
 505 soil properties are 12×12m limited by the CDEF rectangle (noted as  $RF_{other}$ ).  
 506  
 507 Concerning the autocorrelation length, the  $L_x$  and  $L_y$  are firstly respectively set to  
 508 40m and 3m as mentioned before. The sensitivity of the  $L_x$  and  $L_y$  to the reliability  
 509 results, is discussed later. As the random field dimension and the autocorrelation  
 510 length are determined, the series term  $S$  of the truncated K-L expansion should be  
 511 evaluated following Eq. (7). For a target error estimate between 10% and 9%, the  
 512 value of  $S$  is estimated to 37 and 17 for respectively  $RF_{\gamma_g}$  and  $RF_{other}$ . The grid size  
 513 of the random fields is set to 0.5m for both the two directions in this paper which can  
 514 guarantee a good accuracy of the generated random fields according to [29].



533

534 These findings are consistent with the study of [15] in which the importance factors  
535 (IF) of each soil property provided by FORM are available. The IF of  $\gamma_g$  varies  
536 between 0.39 and 0.63 in [15] for different failure modes and the IF of  $K_0$  is within a  
537 range of [-0.35, -0.6]. On the contrary, the IFs of the four soil properties ( $c$ ,  $\phi$ ,  $E$ , and  
538  $\nu$ ) are very close to 0 for any failure mode. It is noted that the IFs given in FORM  
539 represent the contribution of the soil property to the failure probability. This is quite  
540 different to the study in this section and the Sobol-based sensitivity analyses (section  
541 2.3.3) which focus on the contribution of each input variable w.r.t. the total variability  
542 of the model response.

543

544 Based on the observations and discussions above, it is reasonable to consider only the  
545 variability of  $K_0$  and  $\gamma_g$ , and to regard the other soil properties ( $c$ ,  $\phi$ ,  $E$ , and  $\nu$ ) as  
546 deterministic in the reliability analysis for the study case. The decrease of the number  
547 of soils properties to be simulated with random fields can reduce the dimension of the  
548 input space and thus significantly reduce the computational time of a meta-modelling  
549 based reliability analysis. The dimension is decreased from 122 which correspond to 6  
550 random fields ( $122=17\times5+37\times1$ ) to 54. It is noted that the adopted assumption which  
551 considers the parameters  $c$ ,  $\phi$ ,  $E$ , and  $\nu$  as deterministic is based on the present  
552 probabilistic soil models (Table 1) and on the parametric study results (Figures 5 and  
553 6). In practice, the statistics of the soil properties can be different to the ones  
554 considered in Table 1. The corresponding contributions to the model response will  
555 then vary.

556



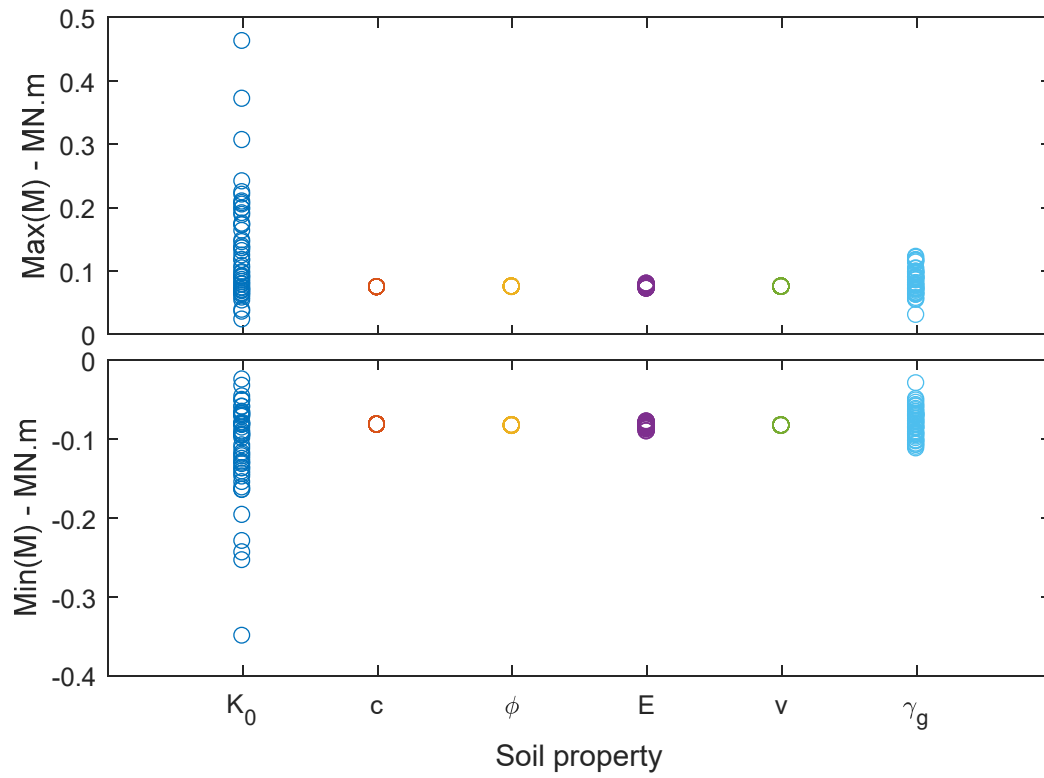


Figure 5 Variation of the max(M) and min(M) w.r.t. the 50 random fields of each soil property

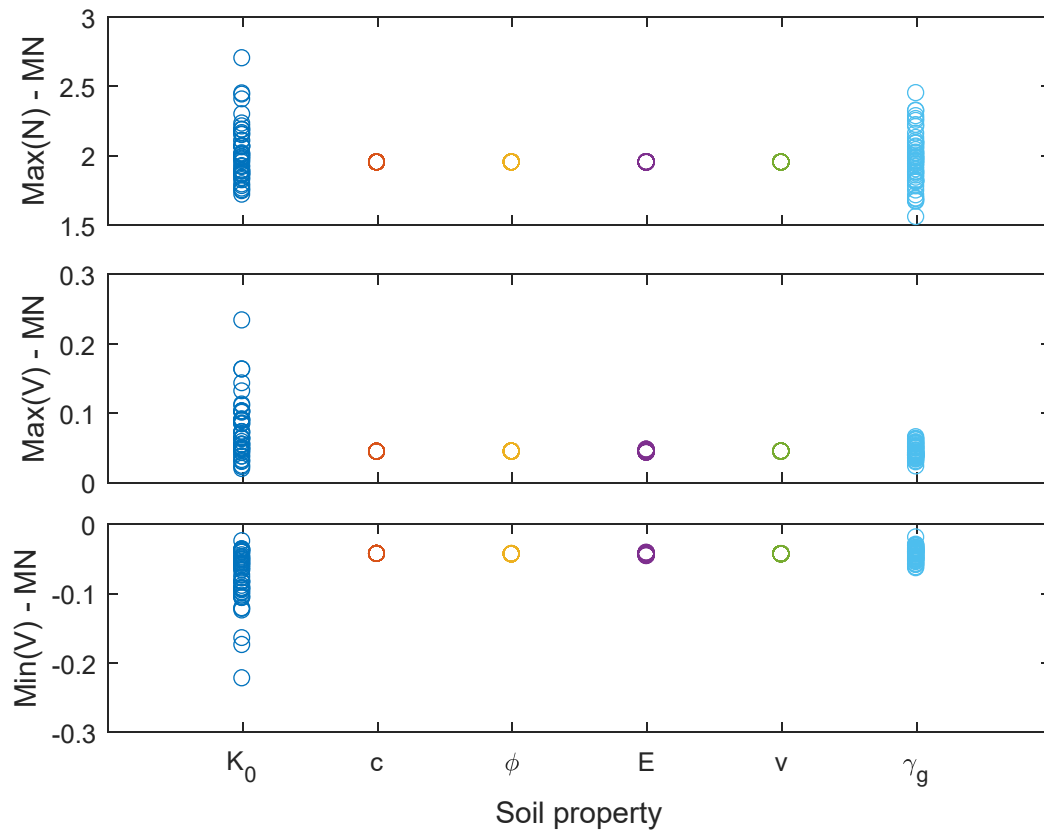


Figure 6 Variation of the max(N), max(V) and min(V) w.r.t. the 50 random fields of each soil property

## 5 Numerical simulations and results

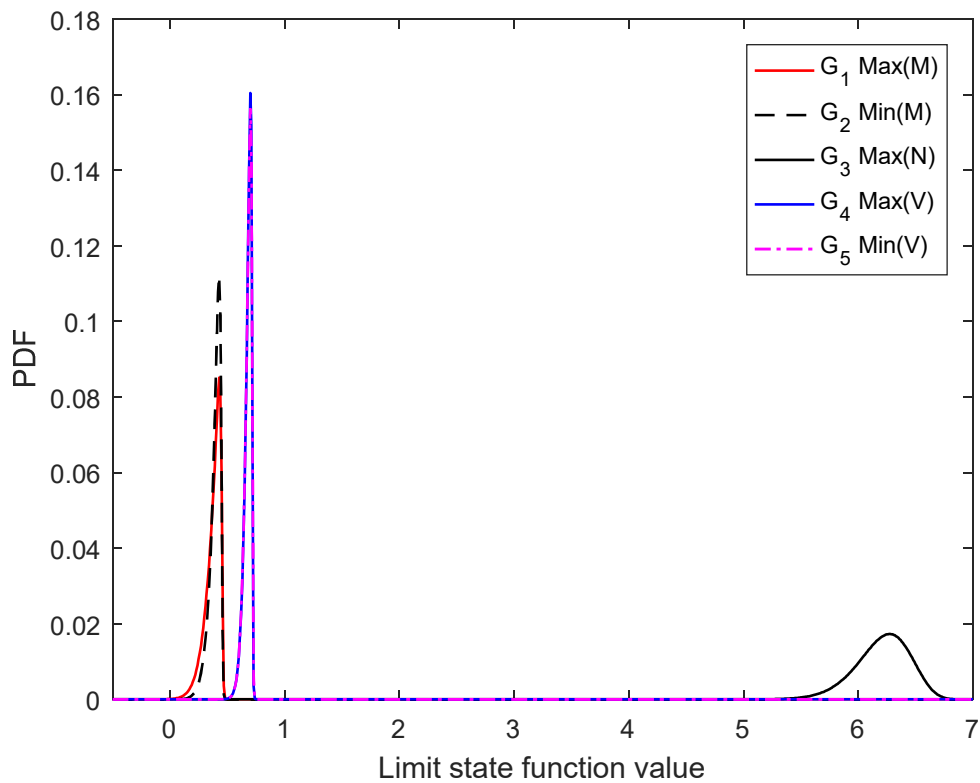
This section aims at presenting the reliability analysis of the studied tunnel lining considering soil spatial variability. Following the conclusion of the previous section, only the  $K_0$  and  $\gamma_g$  are modelled by means of random fields and the other four soil properties are set to a deterministic value (mean value presented in Table 1). The results for a reference case obtained by the method SPCE/GSA are presented and interpreted at first. The reference case refers to the case where autocorrelation lengths are respectively specified to be 40m and 3m for the horizontal and vertical directions, and the two soil properties ( $K_0$  and  $\gamma_g$ ) are simulated by means of random fields following Table 1. Then, the effects of the autocorrelation length are discussed by testing different values for  $L_x$  and  $L_y$ . The effect of considering the soil spatial variability is investigated in the end of the section.

### 5.1 Results of the reference case

The results of the reference case obtained by the SPCE/GSA method are presented in this section. The associated parameters are given previously. Following the procedure presented in the section *Reliability analysis procedure used in the paper*, five 5<sup>th</sup>-order meta-models are constructed for the five failure modes and the reliability results are obtained by performing an MCS with each meta-model. For the performed MCSs, the  $N_{MCS}$  is set to  $1 \times 10^7$ . Such a large MCS running number can ensure that the CoV of the obtained system failure probability is smaller than 5%. Figure 7 shows the probability density function (PDF) of the five limit state functions. Table 2 presents numerically the reliability results in terms of the individual failure probability, system failure probability and the mean and standard deviation of the five extreme internal actions of the tunnel lining.

A quick review of Figure 7 reveals that the  $G_3$  values are very far away from the failure domain ( $G_i < 0$ ) compared to other limit state functions. This indicates that the

588 normal force failure mode is the least likely case among the five individual failure  
589 modes. On the contrast, the values of  $G_1$  and  $G_2$  are close to the failure domain and  
590 their PDF curves show a greater dispersion than those of  $G_4$  and  $G_5$ . This indicates  
591 that the bending moment resistance is probably the most likely failure mode and the  
592 system failure is controlled by the extreme bending moment values. On the basis of  
593 these observations and Figure 7, the failure probabilities associated with the shear  
594 force ( $G_4$  and  $G_5$ ) fall in between those of the bending moment and the normal force.  
595 Furthermore, it is observed that the five PDF curves are not symmetric. They are all  
596 negatively skewed with a relatively large tail in the left. This is because the input  
597 variables are not symmetric and they follow a lognormal distribution.



598  
599 **Figure 7. PDF of the five limit state function values for the reference case**

600 The system failure probability is estimated to  $7.3 \times 10^{-4}$  as presented in Table 2. The  
601 failure probabilities related to  $G_1$  and  $G_2$  are respectively  $7.1 \times 10^{-4}$  and  $2.3 \times 10^{-5}$ . They  
602 are all bigger than the failure probabilities of other failure modes. This confirms the

conclusions made above and exhibits again that the bending failure mode is the most probable case. Particularly, the maximum value of  $\mathbf{M}$  is more critical than the minimum one as revealed by their failure probability. As for the other three failure modes, the relating failure probabilities are all extremely small. Even with a MCS of  $N_{MCS}=1\times 10^8$ , none of the values of  $G_3$ ,  $G_4$  or  $G_5$  are found to be less than 0. As a consequence, the failure probabilities of these three failure modes are all considered to be probably smaller than  $1\times 10^{-6}$ , even maybe smaller than  $1\times 10^{-8}$ . It is not worth determining precisely such small failure probability, given that the calculation time of a MCS for the failure probability smaller than  $1\times 10^{-6}$  is unaffordable even with the constructed meta-model. In addition, these three failure modes are expected to have almost no effect on the system failure probability.

Table 2 also provides the mean and standard deviation of the five internal actions as well as their capacity. For the bending moment, it can be observed that the absolute value of the mean and standard deviation of the  $\max(\mathbf{M})$  are all slightly greater than those of the  $\min(\mathbf{M})$ . This corresponds to the little bigger tail in the left of the  $G_1$  PDF curve compared to the one of  $G_2$  as presented in Figure 7, given that the standard deviation can reflect to some degree the scatter of the data. In contrast to the bending moment, the shear force presents a good agreement in both the mean value (absolute) and standard deviation between  $\max(\mathbf{V})$  and  $\min(\mathbf{V})$ . This corresponds to the almost superposed two PDF curves of  $G_4$  and  $G_5$  in Figure 7. As for the normal force, its standard deviation and the difference between its mean value and its capacity are all the biggest among the five cases.

**Table 2. Reliability results of the studied tunnel lining**

	$\max(\mathbf{M})$ MN.m	$\min(\mathbf{M})$ MN.m	$\max(\mathbf{N})$ MN	$\max(\mathbf{V})$ MN	$\min(\mathbf{V})$ MN	System
Failure probability	$7.1\times 10^{-4}$	$2.3\times 10^{-5}$	$< 1\times 10^{-6}$	$< 1\times 10^{-6}$	$< 1\times 10^{-6}$	$7.3\times 10^{-4}$

Mean	0.126	-0.108	1.992	0.071	-0.072	/
Standard deviation	0.069	0.050	0.239	0.033	0.033	/
Capacity	0.5	-0.5	8.2	0.75	-0.75	/

## 5.2 Influence of the autocorrelation lengths

For a reliability analysis with the **random-fields** approach, the values of autocorrelation length should be selected carefully since they define the autocorrelation structure of random fields [9], [46]. The autocorrelation lengths are set respectively to 40m and 3m in the previous reliability analysis for a conservative design. This section aims at studying the influence of this factor on tunnel lining reliability by testing several values of the autocorrelation length. It should be noted that the series term  $S$  of K-L expansion needs to be re-evaluated for different autocorrelation length values **w.r.t.** the Eq. (7).

Figure 8 plots the system failure probability ( $Pf_{sys}$ ) of the tunnel lining versus different values of the autocorrelation length. The horizontal autocorrelation length ( $L_x$ ) **varies** between 10 and 40m with the vertical autocorrelation length ( $L_y$ ) being fixed to 3m. More results are obtained by varying  $L_y$  between 1.5 and 3m with  $L_x$  being 40m.

From Figure 8, it is found that the  $Pf_{sys}$  decreases with the autocorrelation length decreases. For example, the  $Pf_{sys}$  declines from  $7.29 \times 10^{-4}$  to  $5.77 \times 10^{-5}$  when the  $L_y$  changes from 3m to 1.5m. A smaller autocorrelation length means that the soil is severely non-homogeneous. This implies that the more soil is non-homogeneous, the safer tunnel lining is from the reliability analysis point of view. A possible explanation is as follows. A higher autocorrelation length indicates that the discretised points of the random field are more strongly correlated even separated by a large

651 distance. It therefore results in relatively slow variation in the simulated values of soil  
652 properties and presents a greater chance to form relatively uniform zones during one  
653 random field generation. The representative values of such uniform zones are  
654 stochastic under the prescribed distribution (given in Table 1). As a result, the average  
655 values (the mean of the simulated values for all the stochastic grids of one random  
656 field) among different realizations are not constant but vary more significantly in the  
657 cases of high autocorrelation lengths. For the cases of low autocorrelation lengths, the  
658 average values have a low probability of being very big or very small due to the  
659 presence of heterogeneous areas with dispersed values. In other word, the average  
660 value of the samples generated in the random fields with small autocorrelation length  
661 corresponds to a narrow range of variation. Therefore, lower autocorrelation length  
662 leads to a smaller variability of the system response, and thus a smaller probability of  
663 passing a specified threshold and vice versa. Another remark from Figure 8 is that the  
664 decrease of  $Pf_{sys}$  is more significant when reducing  $L_y$  than  $L_x$ . This indicates that the  
665 vertical autocorrelation length  $L_y$  has a greater impact on the tunnel lining reliability  
666 than the horizontal one.

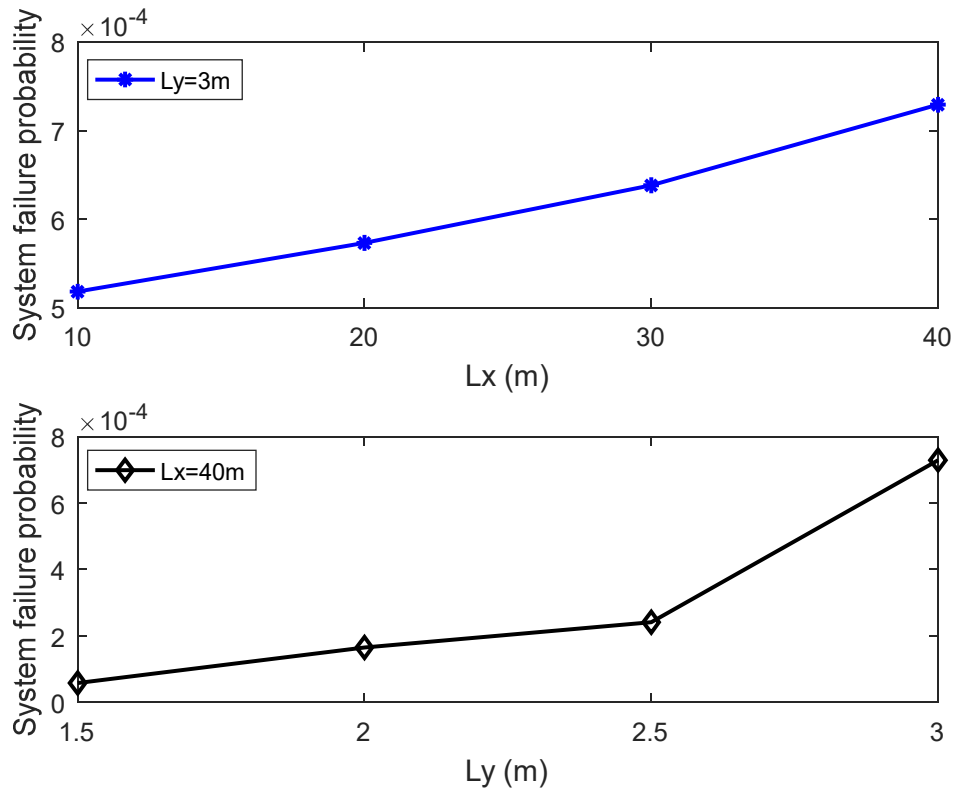


Figure 8. Effect of the autocorrelation length on the system failure probability of the tunnel lining

### 5.3 Effect of taking into account the soil spatial variability

The soil spatial variability is simulated by the random field theory and is taken into account for the reliability analyses in this paper. Different values of one soil parameter are generated and assigned to different points of the random field for one deterministic calculation instead of the assumption of homogeneous soils adopted in [15]. The purpose of this section is to discuss the effect of considering the soil spatial variability on the tunnel lining reliability. Complementary reliability analysis is thus performed in this section in which the two soil properties ( $K_0$  and  $\gamma_g$ ) are modeled by means of random variables with the distribution parameters given in Table 1. The obtained results are compared with the cases of random fields.

Figure 9 presents the system failure probabilities with different values of autocorrelation lengths together with the case of random variables. It is observed that

the failure probability obtained in the case of random variables is higher than the one of any **random-fields** case. The value is increased from  $7.29 \times 10^{-4}$  in the reference case to  $2.66 \times 10^{-3}$  in the case of random variables. Therefore, ignoring the soil spatial variability may induce a higher failure probability and thus a conservative design. In fact, using random variables to simulate the soil variability is based on the assumption that two arbitrary points of the field are perfectly correlated i.e. the soil is homogeneous. It corresponds to an extreme case in which the horizontal and vertical autocorrelation lengths are both equal to infinite. This characteristic eliminates the variability within one calculation but increases the uncertainty in the global average value from one calculation to another. The variance of the model response is thus increased.

As a conclusion of the comparison study shown in Figure 9, the **random-variables** approach which neglects totally the soil spatial variability can be performed at a first stage to provide an upper bound for failure probability. On the other hand, it exists also a second way to take into account the effect of the soil spatial variability in reliability analysis. It assumes the soil to be homogeneous but with a reduced variance compared to the original distribution parameter. Such a simplified approach can replace the **random-fields approach** to predict the variation of the system response and failure probability. It has been widely applied in the field of slope stability as suggested by [47], [48]. The reduction factor can be determined with a typical failure length and autocorrelation distance. However, it should be noted that the results provided by this simplified approach could be questionable with highly variant soil properties or small autocorrelation distances.



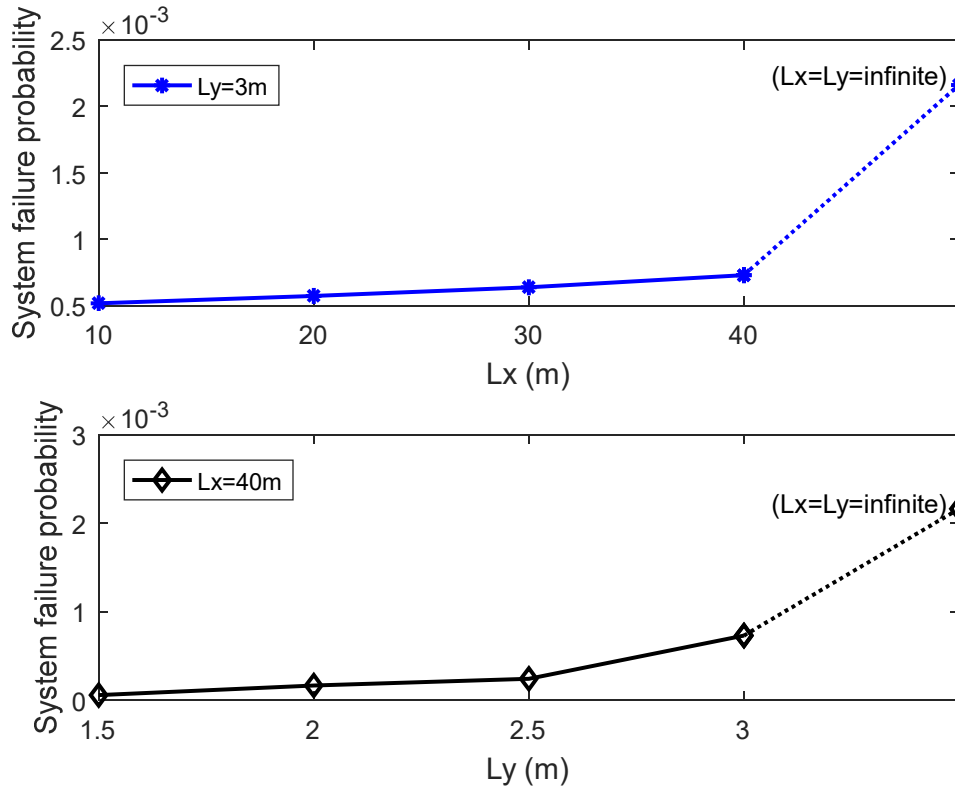


Figure 9. Effect of considering the soil spatial variability on the system failure probability

## 6 Discussions

Two points about the present study are discussed in this section. The first one focuses on the computational efficiency of the method SPCE/GSA which is highlighted by comparing with using a direct Monte Carlo Simulation (MCS) for the present problem. The second one aims at comparing the results obtained by the SPCE with the previous work of [15] in terms of failure probability and the sensitivity index of each soil property.

### 6.1 Computational efficiency

In the event that a direct MCS is employed to perform the reliability analysis for the case of random fields ( $P_f = 7.3 \times 10^{-4}$ ), at least 547 546 model evaluations are needed for a target error  $CoV_{P_f} = 5\%$  according to Eq. (12). On the contrary, the SPCE/GSA method needs only 2000 calls to the deterministic model for constructing

the meta-models. This could lead to a significant decrease of the computational time of the reliability analysis, saying from 15 days to 2 hours given than running one deterministic calculation and generating one realisation of the two random fields use around 2.5 seconds in an Intel Xeon CPU E5-2609 v4 1.7GHz (2 processors) PC. It indicates that using a direct MCS to analyse the stochastic problems with a low  $Pf$  is very time-consuming even with a simplified deterministic model such as the HRM. Applying an alternative method to reduce the computational burden for such problems is thus useful. The SPCE/GSA, introduced in this paper, could be a good choice since it is efficient and can provide a variety of interesting results.

## 6.2 Comparison with the previous work

The purpose of this section is to compare the obtained reliability results (e.g. failure probability and sensitivity index) with the ones published in [15] which studied also the tunnel lining but with means of random variables.

In this section, the six soil properties are modelled by means of independent random variables as the works in [15].  $N_{ED}$  standard normal vectors with the dimension of 6 are generated at first. Then, they are transformed to specific random variables (physical values of the six soil properties) following the probabilistic distribution and statistics given in Table 1. The associated tunnel lining internal actions are evaluated using the HRM for each set of the six soil properties. Based on the model evaluations and the  $N_{ED}$  standard normal vectors, five 5<sup>th</sup>-order SPCE meta-models are constructed respectively for the five failure modes. The system failure probability can be estimated by performing five MCSs w.r.t. the meta-models. Table 3 presents the obtained result and compares it with the one published in [15] which was estimated by a direct MCS. It is observed that the system failure probability obtained by the SPCE is  $2.82 \times 10^{-3}$ . This value represents a good agreement with the result of [15] which can be regarded as a standard reference since the direct MCS was employed. Note that

around 200 calls to the deterministic model are required for this analysis using the SPCE while it is at least necessary 5000 model evaluations to reach a converged MCS result as mentioned in [15]. In conclusion, the method SPCE is efficient and is able to provide an accurate estimate of the failure probability of the tunnel lining.

**Table 3. Comparison of the system failure probability obtained in this paper with the one in [15]**

Method	This paper	Kroetz et al. [15]
	SPCE	Direct MCS
Failure probability	$2.82 \times 10^{-3}$	$3.01 \times 10^{-3}$

In addition, the SPCE method has the capacity to provide the Sobol index of each input random variable by simply post-processing the SPCE coefficients as mentioned in section 2.3.3. It allows knowing the contribution of each soil property to the variability of the **lining forces**. Figure 10 presents the obtained Sobol **indices** for the five failure modes. It clearly shows that the two most important parameters are always  $K_0$  and  $\gamma_g$  for all the individual failure modes. The sum of the Sobol index of these two variables is close to 1, which means that the response variability is almost induced completely by these two soil properties. As for the other soil properties, they are considered to have non-significant influences on the variability of the results, since the corresponding Sobol indices are all smaller than 0.02. In [15], the importance factors (IF) of each soil property provided by FORM are available as mentioned before. The IF of  $\gamma_g$  is varied between 0.39 and 0.63 in [15] for different failure modes and the IF of  $K_0$  varies within a range of [-0.35, -0.6]. These values are different from the ones shown in Figure 10. This observation is not surprising since the sensitivity index of Figure 10 represents the contribution of each soil property to the response variability, while the IF computed by FORM measures the contribution to the failure probability. On the contrary, the IFs of the four other soil properties ( $c$ ,  $\varphi$ ,  $E$ , and  $\nu$ ) are very close to 0 for any failure mode. This finding is consistent with the

present study. Therefore, for the response variability or the failure probability, the impact of the four parameters ( $c$ ,  $\phi$ ,  $E$ , and  $\nu$ ) is negligible. They can thus be treated as deterministic in reliability analyses at least in the context of random variables.

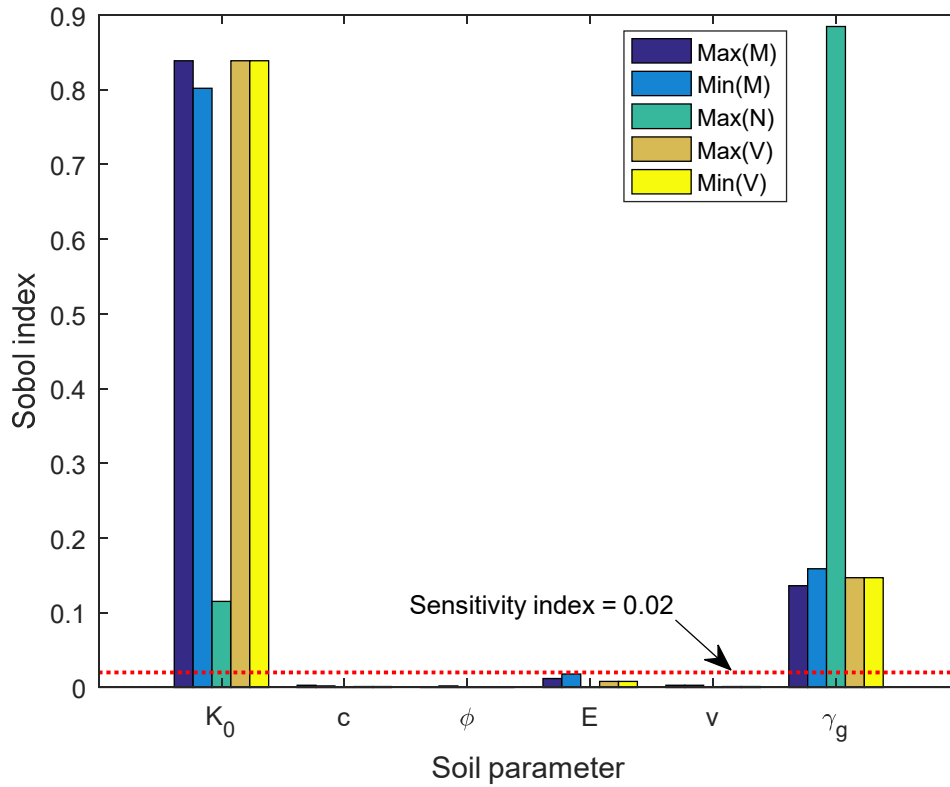


Figure 10. Sobol index of each soil property for the five failure modes

## 7 Conclusion

In this paper, reliability analysis of a circular tunnel lining is presented. The soil spatial variability is considered in the study and is simulated by the random field theory. The individual and system failure probabilities of the studied tunnel lining are provided by using a metamodeling technique SPCE/GSA combined with the HRM. The main conclusions can be listed as follows.

1. The  $K_0$  and  $\gamma_g$  are the two most important soil properties for the tunnel lining reliability under the condition of the assumed soil probabilistic model. This finding is thereafter used to reduce the number of input variables when dealing

with spatially varying soils. In practice, one can identify the significant soil properties for the encountered specific soil conditions by performing a parametric study as shown in section 4.

2. The system failure of the tunnel lining is mainly controlled by the bending failure mode. Particularly, the maximum value of the bending moment in the tunnel lining is the most critical internal action. On the contrary, the largest safety margin is found for the normal load limit state.
3. The soil spatial variability has an important effect on the tunnel lining reliability. Using the **random-variables** approach, in which the soil spatial variability is ignored, can lead to much greater failure probability compared to the **random-fields approach**. This indicates the importance of accounting for the soil spatial variability in reliability analysis of a tunnel lining.
4. The autocorrelation length, which defines the covariance between two arbitrary points in a random field, has also a significant influence on the tunnel lining reliability. The higher autocorrelation length is, the greater failure probability becomes. In particular, the reliability results are more sensitive to the vertical autocorrelation length than the horizontal one. These observations indicate the importance of determining the autocorrelation length values. However, there is usually not enough measurement data in practice which allows obtaining meaningful statistical estimates. The solution is then to determine these values by measurements of the site in the vicinity or from the literature. For such case, a large value for the autocorrelation length is recommended since it leads to conservative designs, as demonstrated in this paper and reported in [9], [46], [49].

These conclusions demonstrate that the present technique is able to provide efficient solutions for determining the failure probability of a tunnel lining and performing

parametric studies. Hence, it can be used for the reliability-based design of the tunnel lining in a preliminary stage.

## 8 Acknowledgement

The first two authors thank gratefully the China Scholarship Council for providing them PhD Scholarships for their research works.

## 9 References

- [1] G. Mollon, D. Dias, and A.-H. Soubra, “ Probabilistic Analysis of Circular Tunnels in Homogeneous Soil Using Response Surface Methodology,” *J. Geotech. Geoenvironmental Eng.*, vol. 135, no. 9, pp. 1314–1325, 2009.
- [2] G. Mollon, D. Dias, and A. H. Soubra, “Probabilistic Analysis and Design of Circular Tunnels against Face Stability,” *Int. J. Geomech.*, vol. 9, no. 6, pp. 237–249, 2009.
- [3] H. Li and B. K. Low, “Reliability analysis of circular tunnel under hydrostatic stress field,” *Comput. Geotech.*, vol. 37, no. 1–2, pp. 50–58, 2010.
- [4] A. T. C. Goh and W. Zhang, “Reliability assessment of stability of underground rock caverns,” *Int. J. Rock Mech. Min. Sci.*, vol. 55, pp. 157–163, 2012.
- [5] G. Mollon, D. Dias, and A.-H. Soubra, “Probabilistic Analysis of Pressurized Tunnels against Face Stability Using Collocation-Based Stochastic Response Surface Method,” *J. Geotech. Geoenvironmental Eng.*, vol. 137, no. 4, pp. 385–397, 2011.
- [6] H. Zhao, Z. Ru, X. Chang, S. Yin, and S. Li, “Reliability analysis of tunnel using least square support vector machine,” *Tunn. Undergr. Sp. Technol.*, vol. 41, pp. 14–23, 2014.
- [7] Q. Wang, H. Fang, and L. Shen, “Reliability analysis of tunnels using a metamodeling technique based on augmented radial basis functions,” *Tunn.*

- 840 *Undergr. Sp. Technol.*, vol. 56, pp. 45–53, 2016.
- 841 [8] A. Hamrouni, D. Dias, and B. Sbartai, “Reliability analysis of shallow tunnels  
842 using the response surface methodology,” *Undergr. Sp.*, vol. 2, no. 4, pp. 246–  
843 258, 2017.
- 844 [9] Q. Pan and D. Dias, “Probabilistic evaluation of tunnel face stability in  
845 spatially random soils using sparse polynomial chaos expansion with global  
846 sensitivity analysis,” *Acta Geotech.*, vol. 12, no. 6, pp. 1415–1429, 2017.
- 847 [10] P. Zeng, S. Senent, and R. Jimenez, “Reliability Analysis of Circular Tunnel  
848 Face Stability Obeying Hoek–Brown Failure Criterion Considering Different  
849 Distribution Types and Correlation Structures,” *J. Comput. Civ. Eng.*, vol. 30,  
850 no. 1, p. 04014126, 2016.
- 851 [11] H. . Hong, “An efficient point estimate method for probabilistic analysis,”  
852 *Reliab. Eng. Syst. Saf.*, vol. 59, no. 3, pp. 261–267, 1998.
- 853 [12] Y.-G. Zhao and T. Ono, “New Point Estimates for Probability Moments,” *J.*  
854 *Eng. Mech.*, vol. 126, no. 4, pp. 433–436, 2000.
- 855 [13] G. F. Napa-García, A. T. Beck, and T. B. Celestino, “Reliability analyses of  
856 underground openings with the point estimate method,” *Tunn. Undergr. Sp.*  
857 *Technol.*, vol. 64, no. Apr., pp. 154–163, 2017.
- 858 [14] Q. Lü, Z. P. Xiao, J. Ji, and J. Zheng, “Reliability based design optimization for  
859 a rock tunnel support system with multiple failure modes using response  
860 surface method,” *Tunn. Undergr. Sp. Technol.*, vol. 70, no. August 2016, pp.  
861 1–10, 2017.
- 862 [15] H. M. Kroetz, N. A. Do, D. Dias, and A. T. Beck, “Reliability of tunnel lining  
863 design using the Hyperstatic Reaction Method,” *Tunn. Undergr. Sp. Technol.*,  
864 vol. 77, no. March, pp. 59–67, 2018.
- 865 [16] S. M. Dasaka and L. M. Zhang, “Spatial variability of in situ weathered soil,”  
866 *Géotechnique*, vol. 62, no. 5, pp. 375–384, 2012.
- 867 [17] X. Guo, D. Dias, C. Carvajal, L. Peyras, and P. Breul, “Reliability analysis of

- embankment dam sliding stability using the sparse polynomial chaos expansion,” *Eng. Struct.*, vol. 174, no. November, pp. 295–307, 2018.
- [18] H. Duddeck and J. Erdmann, “Structural design models for tunnels in soft soil,” *Undergr. Sp. (United States)*, vol. 9:5-6, pp. 246–259, 1985.
- [19] Takano Y. H., “Guidelines for the design of shield tunnel lining,” *Tunn. Undergr. Sp. Technol.*, vol. 15, no. 3, pp. 303–331, Jul. 2000.
- [20] P. P. Oreste, “A numerical approach to the hyperstatic reaction method for the dimensioning of tunnel supports,” *Tunn. Undergr. Sp. Technol.*, vol. 22, no. 2, pp. 185–205, Mar. 2007.
- [21] N.-A. Do, D. Dias, P. Oreste, and I. Djeran-Maigre, “The behaviour of the segmental tunnel lining studied by the hyperstatic reaction method,” *Eur. J. Environ. Civ. Eng.*, pp. 1–22, Jan. 2014.
- [22] D. C. Du, D. Dias, N. A. Do, and P. P. Oreste, “Hyperstatic Reaction Method for the Design of U-Shaped Tunnel Supports,” *Int. J. Geomech.*, vol. 18, no. 6, pp. 1–12, 2018.
- [23] N.-A. Do and D. Dias, “Tunnel lining design in multi-layered grounds,” *Tunn. Undergr. Sp. Technol.*, vol. 81, pp. 103–111, Nov. 2018.
- [24] D. Du, D. Dias, and N. Do, “Designing U-shaped tunnel linings in stratified soils using the hyperstatic reaction method,” *Eur. J. Environ. Civ. Eng.*, pp. 1–18, Nov. 2018.
- [25] K. Huebner, D. Dewhirst, D. Smith, and T. Byrom, *The finite element method for engineers*. New York: John Wiley and Sons, Inc., 2001.
- [26] G. B. Baecher and J. T. Christian, *Reliability and Statistics in Geotechnical Engineering*. John Wiley & Sons, 2005.
- [27] B. Sudret and A. Der Kiureghian, “Stochastic finite element methods and reliability. A state-of-the-art-report,” University of California, 2000.
- [28] K. K. Phoon, “Numerical recipes for reliability analysis – a primer,” in *Reliability-Based Design in Geotechnical Engineering*, K.-K. Phoon and J.



- 896 Ching, Eds. CRC Press, 2008, p. 545.
- 897 [29] C.-C. Li and A. Der Kiureghian, “Optimal discretization of random fields,” *J.*  
898 *Eng. Mech.*, vol. 119, no. 6, pp. 1136–1154, 1993.
- 899 [30] S. E. Cho and H. C. Park, “Effect of spatial variability of cross-correlated soil  
900 properties on bearing capacity of strip footing,” *Int. J. Numer. Anal. Methods*  
901 *Geomech.*, vol. 34, no. March, pp. 1–26, 2010.
- 902 [31] T. Al-bittar and A.-H. Soubra, “Efficient sparse polynomial chaos expansion  
903 methodology for the probabilistic analysis of computationally-expensive  
904 deterministic models,” *Int. J. Numer. Anal. Methods Geomech.*, vol. 38, no. 12,  
905 pp. 1211–1230, 2014.
- 906 [32] G. Blatman and B. Sudret, “Adaptive sparse polynomial chaos expansion based  
907 on least angle regression,” *J. Comput. Phys.*, vol. 230, no. 6, pp. 2345–2367,  
908 2011.
- 909 [33] G. Blatman and B. Sudret, “An adaptive algorithm to build up sparse  
910 polynomial chaos expansions for stochastic finite element analysis,”  
911 *Probabilistic Eng. Mech.*, vol. 25, no. 2, pp. 183–197, 2010.
- 912 [34] G. Blatman and B. Sudret, “Sparse polynomial chaos expansions and adaptive  
913 stochastic finite elements using a regression approach,” *Comptes Rendus*  
914 *Mécanique*, vol. 336, no. 6, pp. 518–523, 2008.
- 915 [35] B. Sudret, “Polynomial Chaos Expansions and Stochastic Finite Element  
916 Methods,” in *Risk and Reliability in Geotechnical Engineering*, K.-K. Phoon  
917 and J. Ching, Eds. CRC Press, 2014, pp. 265–300.
- 918 [36] Q. Pan and D. Dias, “Sliced inverse regression-based sparse polynomial chaos  
919 expansions for reliability analysis in high dimensions,” *Reliab. Eng. Syst. Saf.*,  
920 vol. 167, no. Nov., pp. 484–493, 2017.
- 921 [37] B. Sudret, “Global sensitivity analysis using polynomial chaos expansions,”  
922 *Reliab. Eng. Syst. Saf.*, vol. 93, no. 7, pp. 964–979, 2008.
- 923 [38] I. M. Sobol’, “Global sensitivity indices for the investigation of nonlinear

- mathematical models,” *Mat. Model.*, vol. 17, no. 9, pp. 43–52, 2005.
- [39] X. Guo, D. Dias, C. Carvajal, L. Peyras, and P. Breul, “A comparative study of different reliability methods for high dimensional stochastic problems related to earth dam stability analyses,” *Eng. Struct.*, vol. 188, no. March, pp. 591–602, 2019.
- [40] J. Perchat, *Traité de béton armé selon l’Eurocode 2*, 3rd ed. Le Moniteur, 2017.
- [41] K.-K. Phoon and F. H. Kulhawy, “Characterization of geotechnical variability,” *Can. Geotech. J.*, vol. 36, no. 4, pp. 612–624, 1999.
- [42] K.-K. Phoon and F. H. Kulhawy, “Evaluation of geotechnical property variability,” *Can. Geotech. J.*, vol. 36, no. 4, pp. 625–639, 1999.
- [43] H. El-Ramly, N. R. Morgenstern, and D. M. Cruden, “Probabilistic stability analysis of a tailings dyke on presheared clay-shale,” *Can. Geotech. J.*, vol. 40, pp. 192–208, 2003.
- [44] S.-H. Jiang, D.-Q. Li, L.-M. Zhang, and C.-B. Zhou, “Slope reliability analysis considering spatially variable shear strength parameters using a non-intrusive stochastic finite element method,” *Eng. Geol.*, vol. 168, no. 86, pp. 120–128, 2014.
- [45] T. Al-bittar, “Probabilistic analysis of shallow foundations resting on spatially varying soils,” Université de Nantes, 2012.
- [46] S. Cho, “Probabilistic Assessment of Slope Stability That Considers the Spatial Variability of Soil Properties,” *J. Geotech. Geoenvironmental Eng.*, vol. 136, no. 7, pp. 975–984, 2009.
- [47] H. F. Schweiger and G. M. Peschl, “Reliability analysis in geotechnics with the random set finite element method,” *Comput. Geotech.*, vol. 32, no. 6, pp. 422–435, Sep. 2005.
- [48] R. Suchomel and D. Mašín, “Comparison of different probabilistic methods for predicting stability of a slope in spatially variable  $c$ - $\phi$  soil,” *Comput. Geotech.*, vol. 37, no. 1–2, pp. 132–140, 2010.

952 [49] L. L. Liu, Y. M. Cheng, and S. H. Zhang, “Conditional random field reliability  
953 analysis of a cohesion-frictional slope,” *Comput. Geotech.*, vol. 82, pp. 173–  
954 186, 2017.  
955